

Keratin19 promotes pancreatic cancer progression and poor prognosis via activating the Hedgehog pathway

CHANGSHENG ZHOU¹⁻⁵, YI XIANG², YANTAO REN^{1,3-5}, MING LI⁶, XIN GOU² and WENGANG LI^{1,3-5}

¹School of Medicine, Xiamen University, Xiamen, Fujian 361102; ²Department of Hepatobiliary Surgery, Guizhou Provincial People's Hospital, Guiyang, Guizhou 550002; ³Department of Hepatobiliary Surgery, Xiang'an Hospital of Xiamen University, School of Medicine, Xiamen University; ⁴Cancer Research Center of Xiamen University, School of Medicine, Xiamen University; ⁵Retroperitoneal Tumor Research Center of The Oncology Chapter of The Chinese Medical Association, School of Medicine, Xiamen University, Xiamen, Fujian 361102; ⁶Xiamen Medicine Research Institute, Xiamen, Fujian 361005, P.R. China

Received November 8, 2022; Accepted January 19, 2023

DOI: 10.3892/ijo.2023.5491

Abstract. Pancreatic cancer is a serious threat to human health, with strong invasiveness, rapid progression and poor prognosis. Tumors expressing keratin 19 (K19) have stronger invasiveness and a worse prognosis. However, the role and mechanism of K19 in pancreatic cancer have remained largely elusive. In the present study, K19 expression was detected in pancreatic cancer tissues, its effect on proliferation, apoptosis and metastasis of pancreatic cancer at the cellular, *in vivo* preclinical and clinical levels was evaluated and its effect on the Hedgehog pathway was analyzed. K19 was significantly overexpressed in pancreatic cancer, promoted pancreatic cancer proliferation and metastasis, inhibited tumor cell apoptosis and was associated with poor prognosis. Mechanistically, these effects were mediated through the activation of the Hedgehog pathway. In conclusion, K19 may be a novel target molecule for pancreatic cancer treatment.

Introduction

Pancreatic cancer, particularly pancreatic head cancer, seriously threatens human health, with high malignancy and poor prognosis (1). At present, the treatment of pancreatic cancer is still mainly based on surgical tumor resection. However, the operation is associated with large trauma and numerous complications, and the postoperative tumor recurrence rate is high. Furthermore, at the time of diagnosis, numerous patients have already missed the opportunity of surgical tumor resection. Thus, the mortality rate is high and the prognosis is poor for patients with pancreatic cancer (1,2). Therefore, it is essential to find new treatment options.

Targeted therapy has been used in the clinical treatment of certain tumors and has achieved a good therapeutic effect (3-5). However, for numerous tumor types, particularly pancreatic cancer, effective targeted therapies are limited. Therefore, further research on pancreatic cancer targeted therapy is required.

The key to effective targeted therapy lies in the selection of target molecules. Therefore, to establish effective targeted therapy for pancreatic cancer, it is first required to find potential effective target molecules.

Keratin 19 (K19), with a molecular weight of ~40 kDa, is a type I cytokeratin but lacks the common tail domain of cytokeratin (6). It has been suggested that K19 is related to the degree of malignancy, invasiveness and poor prognosis of tumors (7). Indeed, tumors expressing K19 have stronger invasiveness and worse prognosis (8). Therefore, it was assumed that high malignancy, strong invasion and metastasis, and poor prognosis of pancreatic cancer are also related to the expression of K19, and that K19 may be a promoter and potential effective therapeutic target for pancreatic cancer. However, research on K19 and pancreatic cancer is scarce, and the role and mechanism of K19 in pancreatic cancer remain largely elusive.

In the present study, it was reported that K19 was significantly overexpressed in pancreatic cancer; it was indicated to promote pancreatic cancer cell proliferation, tumorigenesis and metastasis, inhibit tumor cell apoptosis and to be associated

Correspondence to: Dr Xin Gou, Department of Hepatobiliary Surgery, Guizhou Provincial People's Hospital, 83 Zhongshandong Road, Guiyang, Guizhou 550002, P.R. China
E-mail: gouxingzsy@126.com

Dr Wengang Li, School of Medicine, Xiamen University, 4221 Xiang'annan Road, Xiamen, Fujian 361102, P.R. China
E-mail: lwg11861@163.com

Abbreviations: K19, keratin 19; PTCH, transmembrane receptor patched; SMO, G protein-coupled-like receptor smoothed; Shh, Sonic hedgehog; Ihh, Indian hedgehog; Gli, glioma-associated oncoproteins; Ctrl, control; sh, short hairpin

Key words: pancreatic cancer, keratin19, progression, prognosis, Hedgehog pathway

with poor prognosis. K19 was determined to activate the Hedgehog pathway to promote pancreatic cancer proliferation and metastasis. In other words, K19 promoted pancreatic cancer progression and poor prognosis. Mechanistically, these effects were mediated through the activation of the Hedgehog pathway. K19 may be a novel target molecule for pancreatic cancer treatment.

Materials and methods

Specimens and clinicopathological data of patients with pancreatic cancer. Specimens with complete clinicopathological data were obtained from patients with pancreatic cancer treated by surgery at Guizhou Provincial People's Hospital (Guiyang, China) between December 2018 and September 2020. All patients provided informed consent. The study received the approval from the Ethics Committee of Guizhou Provincial People's Hospital [Guiyang, China; no. (2021)253] and was conducted in line with the principles of the Helsinki declaration. The clinical diagnosis of pancreatic cancer was based on conventional clinical and histological criteria. The operation principle for all of the patients was tumor resection. In addition, pancreatic cancer tissue microarrays (HPanA060CS04, HPanA120Su02) purchased from Shanghai Outdo Biotech Co., Ltd. were used. Finally, the tissues of 117 patients with pancreatic cancer, including 67 males and 50 females with an average age of 63.81 ± 10.14 years, and the follow-up data of 66 patients, including 37 males and 29 females, with a follow-up time of 1-65 months and an average age of 65.33 ± 9.87 years, were used. The demographic data and clinicopathological characteristics of these patients are provided in Table SI.

Cell lines. The commercialized pancreatic cancer cell lines PANC-1 and MIA-PaCa-2 purchased from Beijing SyngenTech Co., Ltd. and Wuhan AtaGenix Co., Ltd., respectively, were cultivated in DMEM (Hyclone; Cytiva) and RPMI1640 (Hyclone; Cytiva) culture medium, respectively, in a 5% CO₂ incubator at 37°C and saturated humidity of 95%. The culture medium was supplemented with 10% fetal bovine serum (Hyclone; Cytiva), 100 U/ml penicillin and 100 µg/ml streptomycin (Thermo Fisher Scientific, Inc.). The mycoplasma culture test was confirmed to be negative every month.

Mice. Male BALB/c nude mice (nu/nu; age, four weeks; body weight, 15-20 g) were purchased from Beijing Vital River Laboratory Animal Technology Co., Ltd. The mice were maintained under specific pathogen-free conditions with a 12-h light/dark cycle, temperature of $22 \pm 2^\circ\text{C}$ and humidity of 40-60%, and had *ad libitum* access to a regular chow diet and water.

Cell proliferation assay. A cell suspension (5,000 cells/well) was added into a 96-well plate and cultured at 37°C and 5% CO₂ for 24, 48, 72 and 96 h. Next, 10 µl of Cell Counting Kit-8 (CCK8) solution (Dojindo Laboratories, Inc.) was added in line with the kit instructions and incubated at 37°C and 5% CO₂ for 4 h. The optical density at 450 nm was detected by a microplate reader.

Cell transfection. The cells in the exponential growth phase were inoculated into a 6-well plate (50,000 cells/well) and cultured at 37°C with 5% CO₂. Transfection of a lentivirus with an overexpression or knockdown vector for K19 was performed by Lipofectamine™ 2000 (Thermo Fisher Scientific, Inc.) according to the manufacturer's instructions the next day and the medium was replaced with fresh medium 8 h after lentivirus transfection. At 72 h after lentivirus transfection, images of the cells were captured under the fluorescence microscope. The cells were collected and the overexpression and knockdown efficiencies were detected by reverse transcription-quantitative PCR (RT-qPCR) and western blot analysis (Fig. S1).

The short hairpin (sh)RNA sequences (Beijing SyngenTech Co., Ltd.) used to knock down K19 expression were as follows: shK19 (knockdown of K19 gene) sense, 5'-GCCGGACTGAAG AATTGAACC-3' and antisense, 5'-CGAAGGTTCAATTCT TCAGTCCGGC-3'; shCtrl (knockdown control) sense, 5'-AAA CGTGACACGTTCCGGAGAA-3' and antisense, 5'-CGA ATTCTCCGAACGTGTCACGTTT-3'. K19-RNA sequences (Beijing SyngenTech Co., Ltd.) used to overexpress K19 expression were as follows: K19 (overexpression of K19 gene, human, NM-002276) included 10,724 DNA bases; Ctrl (overexpression control, mNeogreen) included 9,581 DNA bases.

RT-qPCR. The transfected cells were collected, RNA was extracted, the absorbance at 260 nm (A260)/A280 value was measured and the RNA concentration was estimated. A small amount of RNA was taken out to determine the RNA quality by agarose gel electrophoresis. RNAs that met the requirements were used and denatured at 65°C for 5 min. After the residual genomic DNA of the product was removed by DNase reaction, RT reagent [Hifair® II 1st Strand cDNA Synthesis SuperMix for qPCR (gDNA digester plus); Yeasen Biotechnology (Shanghai) Co., Ltd.] was added to reverse-transcribe the mRNA and synthesize cDNA according to the manufacturer's instructions. The primers and the cDNA products synthesized by RT were used for real-time qPCR (thermocycling conditions: 95°C for 15 sec, 60°C for 1 min, 95°C for 15 sec) in an ABI Prism 7300 PCR instrument (Applied Biosystems, Inc.) and Hieff® qPCR SYBR Green Master Mix [Low Rox; Yeasen Biotechnology (Shanghai) Co., Ltd.] was used according to the manufacturer's instructions. The expression level of GAPDH was calculated according to the $2^{-\Delta\Delta Cq}$ method (9) and used as a standardization control. The PCR primers were as follows: K19 sense, 5'-TAGAGGTGAAGATCCGCGAC-3' and antisense, 5'-CCGTCTCAAACCTTGGTTCGG-3'; GAPDH sense, 5'-TCAAGAAGGTGGTGAAGCAGG-3' and antisense, 5'-TCAAAGGTGGAGGAGTGGGT-3'.

Immunohistochemistry (IHC). The tissues were routinely dehydrated, embedded in paraffin and sliced. After baking slices at 60°C overnight, the tissue sections were successively dewaxed, hydrated, permeated, sealed, antigen-repaired, incubated with primary antibody at 4°C overnight and secondary antibody at room temperature for 30 min, color-rendered, counterstained with hematoxylin and sealed according to standard protocols. Information about the antibodies is provided in Table SII.

The proportion of cells with positive staining was determined as follows: From each slice, 10 high-power vision fields were randomly selected, the number of positive cells among

100 cells in each high-power vision field was determined, and the average value of the total number of these 10 high-power vision fields was then calculated. From the percentage of positive cells, the positive index was scored as follows: <25%, score 0; 25-50%, score 1; 50-75%, score 2; >75%, score 3.

The staining intensity was rated score 0 if there was no color rendering and three levels from light color to deep color corresponded to scores 1, 2 and 3.

The scores of the positive cell proportion and staining intensity were multiplied to obtain the following categories: Scores 0-2, (-); scores 3-4, (+); scores 5-6, (++) ; scores 7-9, (+++).

The cell density (positive cell number/mm²) was determined as follows: From each slice, 10 high-power vision fields (magnification, x400; area, 0.0788 mm²) were randomly selected, the number of positive cells in each high-power field was counted and the average value of the total number of these 10 high-power fields was then taken.

Western blot analysis. Cell lysis and collection of protein were performed using conventional procedures and detection of total protein content using a BCA protein concentration detection kit (Beyotime Institute of Biotechnology) according to the manufacturer's instructions. The total protein was then subjected to SDS-PAGE (10% gel), membrane transfer to an immobilion[®] PVDF membrane, (Merck KGaA), primary antibody and secondary antibody incubation at 4°C overnight and room temperature for 1 h, respectively, and imaging with Luminol reagent (Santa Cruz Biotechnology, Inc.). GAPDH protein was used as a standardization control. Antibody information is provided in Table SII.

Colony-formation assay. The cells of each experimental group (200 cells/well) were added into a 6-well plate and three duplicate wells were set in each group. The cells were cultured at 37°C with 5% CO₂. The culture medium was changed every 3 days and the cells were observed. After 14 days of culture, 4% paraformaldehyde was added for fixation at room temperature for 10 min. Next, the colonies were stained with crystal violet aqueous solution (Beyotime Institute of Biotechnology) at room temperature for 10 min, images were acquired under a microscope and the number of colonies (clusters of >50 cells) was counted.

Apoptosis assay. Cells of each experimental group (100,000 cells/well) were added into a 24-well plate and three duplicated wells were set in each group. They were incubated at 37°C with 5% CO₂ for 48 h. The cells were collected, Annexin V and propidium iodide [Yeasen Biotechnology (Shanghai) Co., Ltd.] were added and cells were incubated at room temperature in the dark for 15 min and suspended in 1X Binding Buffer [Yeasen Biotechnology (Shanghai) Co., Ltd.] according to the manufacturer's instructions. Apoptosis was then detected by flow cytometry.

Cell cycle analysis. The cells of each experimental group (100,000 cells/well) were added into a 24-well plate and each group was set with three duplicated wells, which were cultured at 37°C with 5% CO₂ for 48 h. The cells were collected and added into ethanol precooled at -20°C and fixed at 4°C

overnight. Next, the ethanol was removed, 300 μl propidium iodide solution (Biolegend, Inc.) was added and the cells were incubated away from light at room temperature for 15 min. The cell cycle was then detected by flow cytometry.

Transwell assay. Transwell chambers (Corning, Inc.; pore size, 8 μm) were inserted into a 24-well plate, cells of each experimental group (20,000 cells/200 μl/chamber) were added to the chamber, and three duplicate wells were set for each group. Next, 600 μl medium was added into the lower chamber and plates were cultured at 37°C and 5% CO₂ for 24 h. The cell culture medium and non-migrating cells in the upper chamber were removed, 4% paraformaldehyde was added for fixation at room temperature for 10 min and crystal violet aqueous solution (Beyotime Institute of Biotechnology) was added to stain the cells that had migrated at room temperature for 10 min. Images of the cells that had migrated were acquired under a microscope and these cells were counted by ImageJ software version Fiji (National Institutes of Health).

The Transwell invasion assay was performed in a similar manner, with the variation that the filter membranes of the Transwell chambers were precoated with Matrigel[®] (BD Biocoat, Inc.).

Construction of pancreatic cancer cells with stable over-expression of K19. PANC-1 pancreatic cancer cells in the exponential growth phase were inoculated into a 6-well plate (50,000 cells/well) and cultured at 37°C with 5% CO₂. The next day, lentivirus overexpressing K19 and their control (Beijing SyngenTech Co., Ltd.; details provided above) were stably transfected according to the manufacturer's instructions. At 8 h after transfection, the medium was renewed with fresh culture medium. At 72 h after transfection, the cells were screened using 2 μg/ml puromycin (Thermo Fisher Scientific, Inc.) and images were acquired under a fluorescence microscope. Next, the cells were cultured to establish pancreatic cancer cells stably overexpressing K19, and their overexpression efficiency was detected by RT-qPCR and western blot analysis (10) (Fig. S2).

Construction of a subcutaneously transplanted tumor model and an abdominal metastasis tumor model of pancreatic cancer in nude mice. A subcutaneously transplanted tumor model and an abdominal metastasis tumor model of pancreatic cancer in nude mice were constructed via subcutaneously and intraperitoneally injecting PANC-1 cells stably overexpressing K19 (n=6 mice) and control cells (n=6 mice) (2x10⁷/ml cells x0.15 ml/mice). Subsequently, the condition of the nude mice was observed and their body weight and tumor size were measured once every 2-3 days. The tumor size was calculated as follows: Tumor volume (mm³)=1/2 x (tumor long diameter x tumor short diameter²). After reaching the endpoint of the experiment, the mice were euthanized by cervical dislocation. The endpoints of the experiment included that animals were dying and unable to move; did not respond to gentle stimuli; had difficulty breathing; had diarrhoea and gatism; lost their ability to eat or drink; exhibited obvious anxiety and restlessness; their body weight was decreased by >20% of that prior to the start of the experiment; the tumor weight exceeded 10% of the animal's own body weight; the maximum diameter

of the subcutaneous tumor in mice was close to 20 mm (not >20 mm); the tumor was ulcerating; the damage area of animal skin was >30% of the whole body surface; and the skin of the animals was infected and purulent. Of note, the experiment with the mice with abdominal metastasis tumors was terminated two weeks after that with the mice with the subcutaneous transplantation tumor. The tumor was dissected and tumor size and tumor weight were measured. Furthermore, the mesentery, liver, lung and tumor tissues of the mice were dissected for subsequent IHC staining and hematoxylin-eosin (H&E) staining according to standard procedures.

TUNEL apoptosis assay. Tumor tissues from subcutaneous transplanted tumors in mice were routinely dewaxed to water in line with the above IHC method. The instructions of the TUNEL kit (cat. no. G1501; Wuhan Servicebio Technology Co., Ltd.) were then followed. The results were expressed as the number of positive cells.

Remedial experiment. When the cells were cultured and in the exponential growth phase, 5 μ M of glioma-associated oncoprotein 1 (Gli1) inhibitor (GANT 58; cat. no. HY-13282; MedChemExpress) was added. Subsequently, the expression of Gli1 and K19 proteins, as well as the proliferation and invasion of pancreatic cancer cells, were detected according to the previously mentioned western blot, CCK8 and Transwell invasion assays.

Statistical analysis. Values are expressed as the mean \pm standard error of the mean for three or more independent experiments, and were analyzed by SPSS version 23.0 (SPSS, Inc.) and GraphPad Prism software version 8.0 (GraphPad Software, Inc.). Student's t-test, the Mann-Whitney U-test, Fisher's exact test, chi-square test and analysis of variance (ANOVA) were used for assessment of statistical significance. Student's t-test, a parametric test, was used for mean comparison between two groups ($n < 30$ and normal distribution). The Mann-Whitney U-test, a non-parametric test, was used for mean comparison between two groups, which were not suitable for Student's t-test. ANOVA, also a parametric test, was used for mean comparison between two or more groups. For comparison of multiple groups, one-way ANOVA was used along with post-hoc multiple-comparisons tests, including least-significant differences, Student-Newman-Keuls and Bonferroni. The chi-squared test, a nonparametric test, was used for rate comparison between two or more groups ($n \geq 40$ and theoretical frequency $T \geq 1$). Fisher's exact test, also a nonparametric test, was used for rate comparison between two or more groups ($n < 40$ or theoretical frequency $T < 1$). Survival was calculated using the Kaplan-Meier method and analyzed by the log-rank test. Significant variables from the univariate analysis were entered into a multivariate analysis using a Cox regression model with forward stepwise selection. Statistical significance was considered if $P < 0.05$.

Results

K19 is significantly overexpressed in pancreatic cancer and is associated with poor prognosis. To observe the effect of K19 on pancreatic cancer, the expression of K19 in pancreatic

cancer and corresponding paracancerous tissues was first detected by IHC. Compared with paracancerous tissues, K19 was significantly overexpressed in pancreatic cancer tissues (Fig. 1A). Of 117 pancreatic cancer samples, 81 (69.23%) were positive [30 (25.64%) were weakly positive (+), 29 (24.79%) were moderately positive (++) and 22 (18.80%) were strongly positive (+++)] and 36 (30.77%) were negative for K19 expression (Fig. 1B). However, there was no association between K19 expression and the demographic and clinicopathological data of the patients with pancreatic cancer, including age, gender, tumor distribution, tumor size, vascular invasion, tumor metastasis, pathological grading and clinical stage (Table SIII). However, the incidence of tumors with a diameter ≤ 2 cm in the K19-positive group was significantly lower than that in the K19-negative group (Table SIII).

Survival analysis indicated that the overall survival, median survival time and average survival time of patients with pancreatic cancer expressing K19 were significantly reduced, compared with those in patients without K19 expression (Fig. 1C). Furthermore, the one-year survival rate, two-year survival rate and three-year survival rate of patients with pancreatic cancer expressing K19 were also significantly reduced, compared with those in patients without K19 expression (Fig. 1C). The five-year survival rate of patients with pancreatic cancer expressing K19 was 0% (Fig. 1C). Compared with those without K19 expression, no patients with pancreatic cancer expressing K19 survived for >3 years (Fig. 1C). These data suggested that K19 was associated with poor prognosis of patients with pancreatic cancer.

In addition, univariate analysis suggested that K19 expression and the pathological grade were unfavorable prognostic factors for pancreatic cancer (Table I). Multivariate analysis (Cox regression) indicated that K19 expression was an independent risk factor for poor prognosis of pancreatic cancer (Table II).

K19 promotes pancreatic cancer proliferation. To observe the effect of K19 on pancreatic cancer cell proliferation, K19-shRNA (knockdown of K19) and K19-RNA vector (overexpression of K19) were first used to knockdown and overexpress the K19 gene in pancreatic cancer cells, respectively. Next, CCK8, colony-formation and flow cytometric assays were performed to examine the proliferation, colony formation and cell cycle progression of pancreatic cancer cells with knockdown and overexpression of K19, respectively. Knockdown of K19 inhibited pancreatic cancer cell proliferation (Fig. 2A), colony formation (Fig. 2B) and cell cycle progression (Fig. 2C), while overexpression of K19 promoted tumor cell proliferation (Fig. 2D), colony formation (Fig. 2E) and cell cycle progression (Fig. 2F). CyclinD1 and c-Myc have important roles in cancer proliferation (11,12). Of note, compared with that in pancreatic cancer with negative K19 expression, the expression of CyclinD1 and c-Myc in pancreatic cancer with positive K19 expression was upregulated (Fig. 3A).

In addition, as presented in Fig. 3B, the tumors in the mice subcutaneously injected with K19-overexpressing PANC-1 cells grew more quickly, were larger and weighed more than those in the control group. Furthermore, the levels of Ki67, CyclinD1 and c-Myc proteins in the tumors in the mice

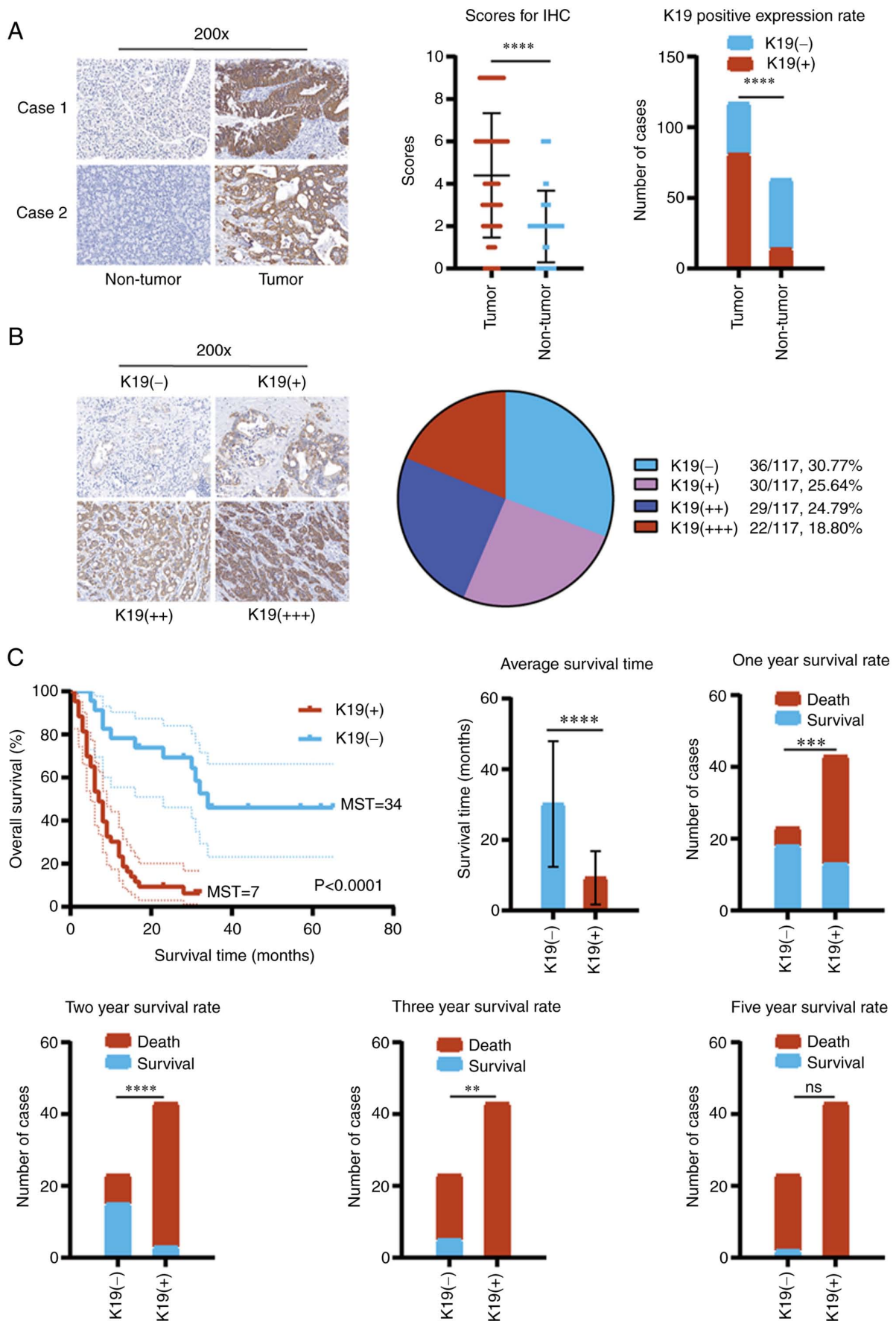


Figure 1. K19 is significantly overexpressed in pancreatic cancer and is associated with poor prognosis. (A) Expression of K19 in pancreatic cancer and corresponding adjacent tissues. K19 was significantly overexpressed in pancreatic cancer tissues (magnification, x200). (B) Different intensity of expression of K19 in pancreatic cancer (magnification, x200). The expression of K19 in pancreatic cancer and corresponding adjacent tissues was detected by immunohistochemistry. (C) K19 decreased the survival of patients with pancreatic cancer. **P<0.01, ***P<0.001, ****P<0.0001; ns, no significance. K19, keratin 19; MST, median survival time.

Table I. Univariate analysis of survival in patients with pancreatic cancer.

Variable	Number of patients	One-year survival, %	Two-year survival, %	Three-year survival, %	Five-year survival, %	P-value
Age, years						0.1824
≤60	24	63	33	8	4	
>60	42	38	24	7	2	
Gender						0.4493
Male	37	43	22	8	3	
Female	29	52	34	7	3	
K19 expression						0.0001
Negative	23	78	65	22	9	
Positive	43	30	7	0	0	
Tumor location						0.0822
Pancreatic head	36	42	19	0	0	
Pancreatic body and tail	17	59	35	24	12	
Pancreas	13	46	38	8	0	
Tumor size, cm						0.5106
≥4	46	50	33	7	4	
>2, <4	17	35	12	6	0	
≤2	3	67	33	0	0	
Vascular invasion						0.3462
Absent	50	50	28	8	4	
Present	16	38	25	6	0	
Lymph node metastasis						0.0906
Absent	43	51	33	12	5	
Present	23	39	17	0	0	
Clinical stage						0.1465
I-II	62	50	29	8	3	
III-IV	4	0	0	0	0	
Pathologic grade						0.0277
I-II	38	61	39	8	3	
III-IV	28	29	11	7	4	

K19, keratin 19.

subcutaneously injected with K19-overexpressing PANC-1 cells were increased (Fig. 3C). Collectively, the above data suggested that K19 promoted pancreatic cancer proliferation, at least in part via enhancing the expression of Ki67, CyclinD1 and c-Myc.

K19 inhibits pancreatic cancer cell apoptosis. To observe the effect of K19 on pancreatic cancer cell apoptosis, flow cytometry was performed. The apoptosis of pancreatic cancer cells with K19 knockdown and K19 overexpression was detected. Knockdown of K19 promoted pancreatic cancer cell apoptosis (Fig. 4A), whereas overexpression of K19 inhibited their apoptosis (Fig. 4B). Bcl-2 has a key role in regulating apoptosis (13,14); i.e., upregulation of Bcl-2 is able to inhibit apoptosis, while downregulation of Bcl-2 may induce apoptosis (15). Therefore, to observe the effect of K19 on the expression of Bcl-2 in pancreatic cancer, IHC was used to detect the expression of Bcl-2 in pancreatic

cancer tissues. As indicated in Fig. 4C, Bcl-2 expression in pancreatic cancer tissues expressing K19 was upregulated as compared with that in pancreatic cancer tissues without K19 expression.

In addition, the results of the TUNEL apoptosis assay suggested that overexpression of K19 inhibited pancreatic cancer apoptosis in the subcutaneous tumors in the mice injected with PANC-1 cells that overexpressed K19 (Fig. 4D). Collectively, these data suggested that K19 inhibited pancreatic cancer cell apoptosis.

K19 promotes pancreatic cancer metastasis. To observe the effect of K19 on pancreatic cancer metastasis, Transwell migration and invasion assays were performed to examine the migration and invasion of pancreatic cancer cells with K19 knockdown and K19 overexpression. As presented in Fig. 5A and B, knockdown of K19 inhibited the migration and invasion of pancreatic cancer cells, while overexpression of

Table II. Independent prognostic factors for survival by multivariate analysis.

Variable	Exp(B) (HR)	SE of Exp(B) (HR)	P-value	95% CI for Exp(B) (HR)
K19 expression	0.200	0.381	<0.001	0.200 (0.095-0.422)
Pathologic grade	1.761	0.292	0.052	1.761 (0.995-3.119)
Tumor location	-	-	0.583	-
Lymph node metastasis	-	-	0.316	-
Clinical stage	-	-	0.291	-
Tumor size	-	-	0.848	-
Vascular invasion	-	-	0.397	-

K19, keratin 19; HR, hazard ratio; SE, standard error.

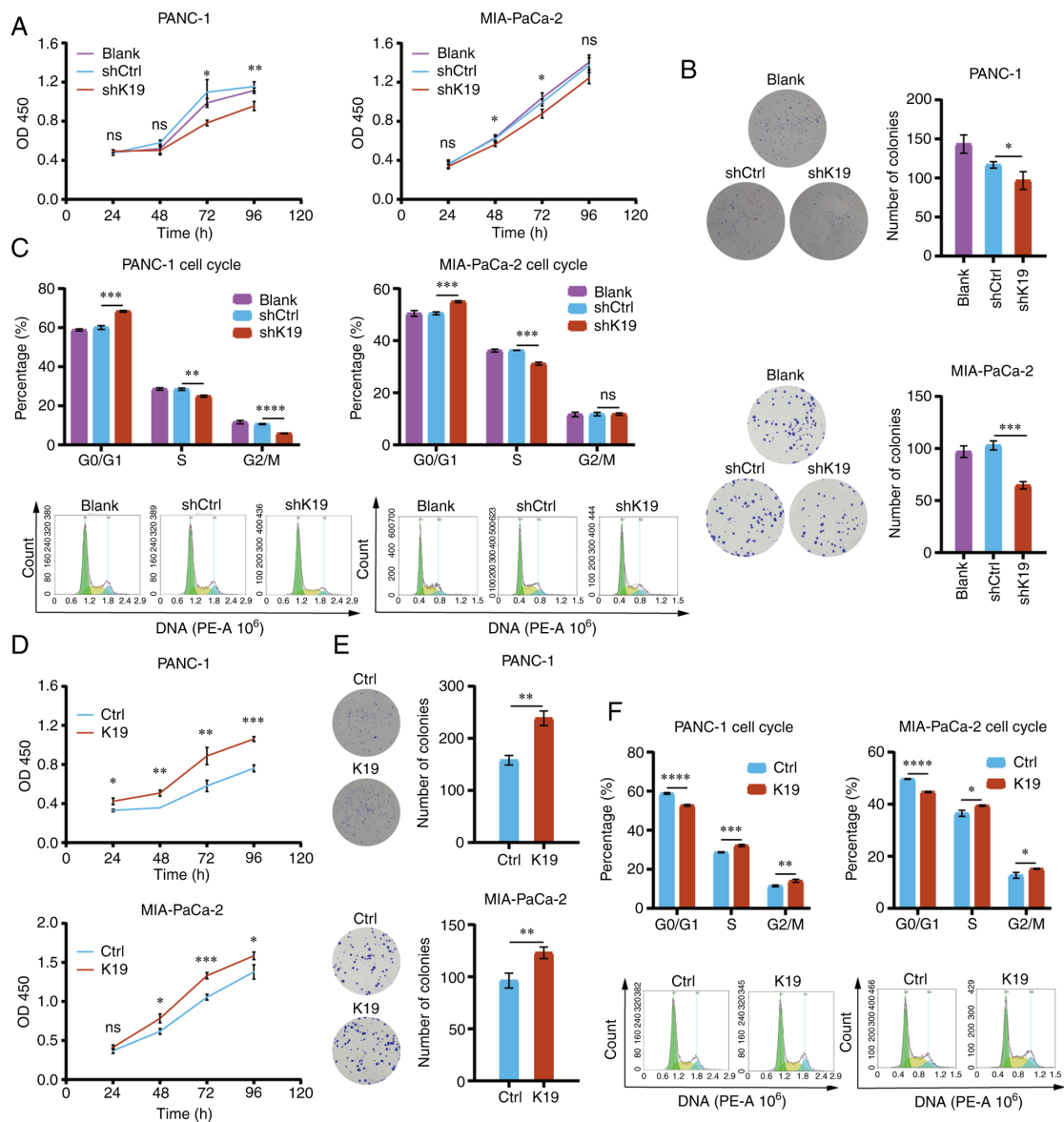


Figure 2. K19 promotes pancreatic cancer cell proliferation *in vitro*. (A) Knockdown of K19 inhibited the proliferation of PANC-1 and MIA-PaCa-2 cells. (B) Knockdown of K19 inhibited the colony formation of PANC-1 and MIA-PaCa-2 cells. (C) Knockdown of K19 inhibited the cell cycle progression of PANC-1 and MIA-PaCa-2 cells. (D) Overexpression of K19 promoted the proliferation of PANC-1 and MIA-PaCa-2 cells. (E) Overexpression of K19 promoted the colony formation of PANC-1 and MIA-PaCa-2 cells. (F) Overexpression of K19 promoted the cell cycle progression of PANC-1 and MIA-PaCa-2 cells. The proliferation, colony formation and cell cycle progression of pancreatic cancer cells with knockdown and overexpression of K19 were detected by Cell Counting Kit-8, clone formation assay and flow cytometry, respectively. These experiments were repeated three times. * $P < 0.05$, ** $P < 0.01$, *** $P < 0.001$, **** $P < 0.0001$; ns, no significance; K19, keratin 19; sh, short hairpin RNA; Ctrl, control; OD, optical density.

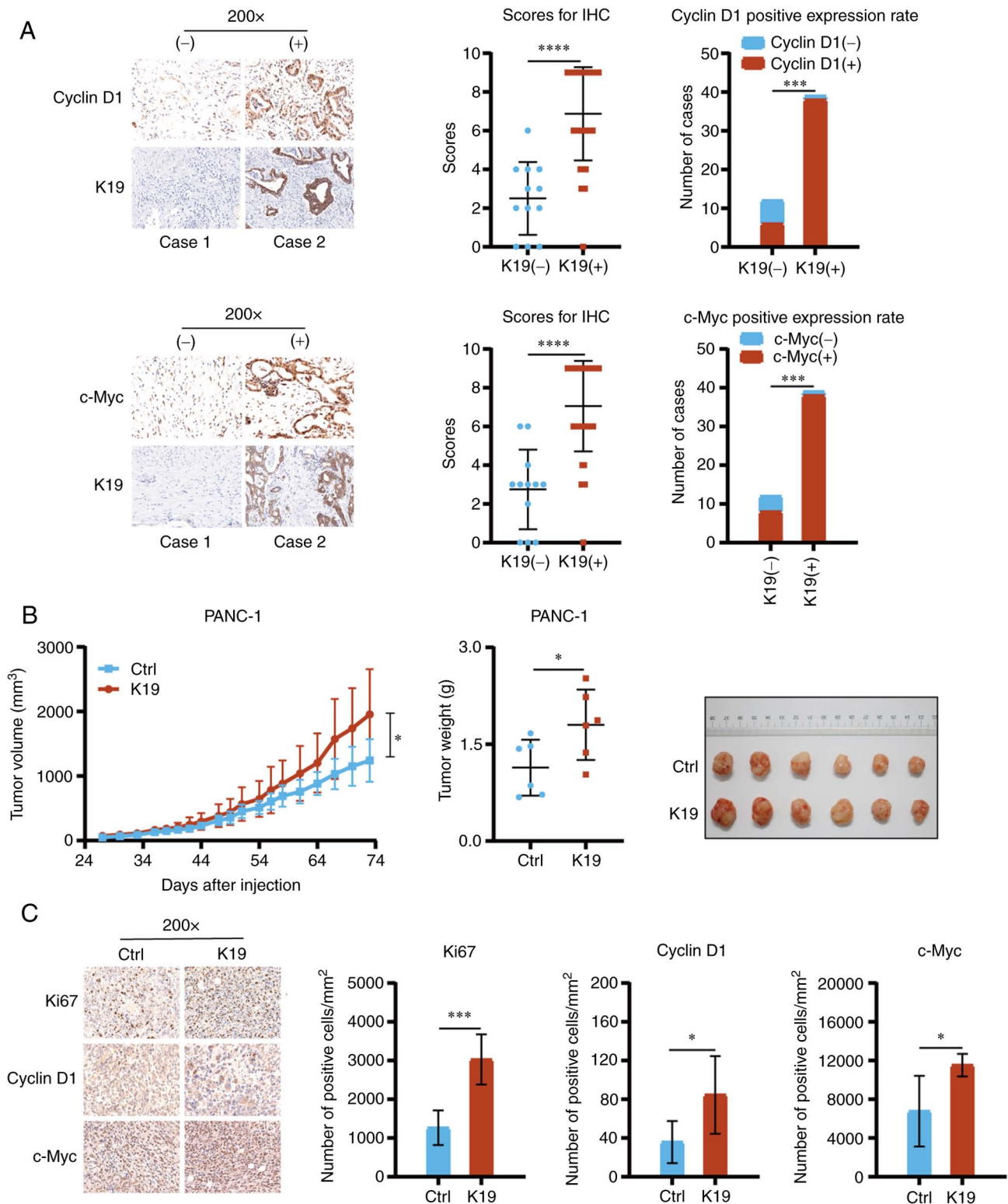


Figure 3. K19 promotes pancreatic cancer proliferation *in vivo*. (A) K19 upregulated the expression of CyclinD1 and c-Myc in pancreatic cancer tissues (magnification, x200). The expression of CyclinD1 and c-Myc in pancreatic cancer tissues with K19-positive and K19-negative status was detected by IHC. (B) Overexpression of K19 promoted the growth of subcutaneous tumors in the mice injected with PANC-1 cells overexpressing K19. (C) Overexpression of K19 promoted the expression of Ki67, CyclinD1 and c-Myc in subcutaneous tumors in the mice injected with PANC-1 cells overexpressing K19 (magnification, x200). The expression of Ki67, CyclinD1 and c-Myc in subcutaneous tumors in the mice injected with PANC-1 cells overexpressing K19 and control was detected by IHC. * $P < 0.05$, *** $P < 0.001$, **** $P < 0.0001$. K19, keratin 19; IHC, immunohistochemistry; Ctrl, control.

K19 promoted their migration and invasion (Fig. 5C and D). MMP2 and MMP9 have important roles in cancer metastasis (16,17). Of note, compared with pancreatic cancer tissues

with negative K19 expression, the expression of MMP2 and MMP9 were upregulated in pancreatic cancer tissues with positive K19 expression (Fig. 5E).

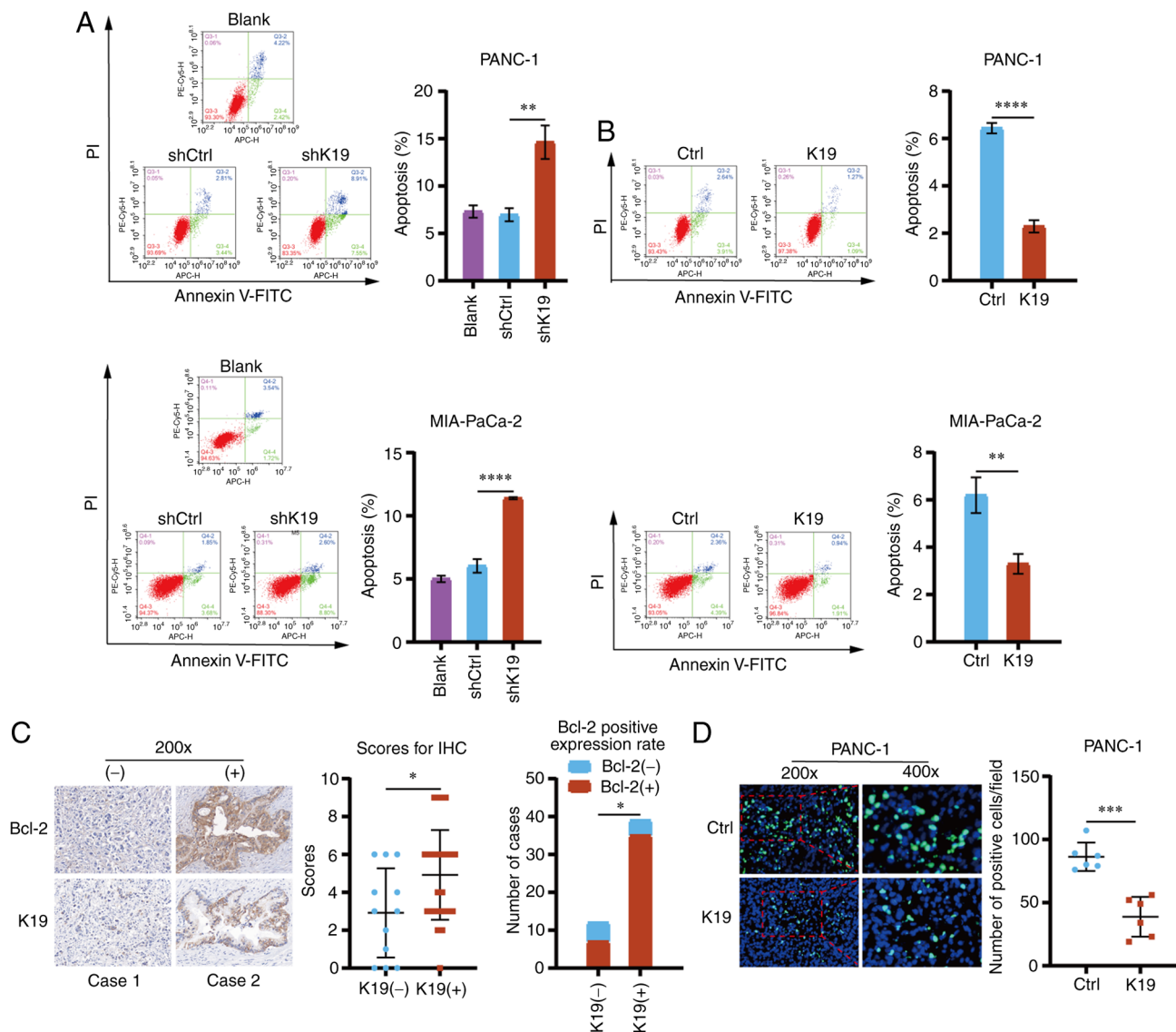


Figure 4. K19 inhibits pancreatic cancer cell apoptosis. (A) Knockdown of K19 promoted apoptosis of PANC-1 and MIA-PaCa-2 cells. (B) Overexpression of K19 inhibited apoptosis of PANC-1 and MIA-PaCa-2 cells. The apoptosis of pancreatic cancer cells with knockdown of K19 and overexpression of K19 was detected by flow cytometry. These experiments were repeated three times. (C) K19 upregulated Bcl-2 expression in pancreatic cancer tissues (magnification, x200). The expression of Bcl-2 in pancreatic cancer tissues with K19 positive and K19 negative status was detected by immunohistochemistry. (D) Overexpression of K19 inhibited tumor cell apoptosis in subcutaneous tumors in the mice injected with PANC-1 cells that overexpress K19 (magnification, x200 in left panels and x400 in magnified windows to the right). The apoptosis of subcutaneous tumors in the mice injected with PANC-1 cells overexpressing K19 and control was detected by a TUNEL apoptosis assay. * $P < 0.05$, ** $P < 0.01$, *** $P < 0.001$, **** $P < 0.0001$. K19, keratin 19; Ctrl, control; sh, short hairpin RNA; PI, propidium iodide.

In addition, overexpression of K19 promoted tumor formation, mesenteric metastasis, liver metastasis and lung metastasis in the mice intraperitoneally injected with K19-overexpressing PANC-1 cells, as compared with the controls (Fig. 5F). Furthermore, the cell density, invasion and infiltration ability of tumor cells were increased in the K19-overexpressing group (H&E; Fig. 5F). Metastatic K19-overexpressing cells were observed in the mesentery, liver and lung tissues on H&E staining (Fig. 5F). In conclusion, the above data indicated that K19 promoted pancreatic cancer metastasis.

K19 activates the Hedgehog pathway and promotes the proliferation and metastasis of pancreatic cancer. The Hedgehog pathway has a key role in pancreatic cancer tumorigenesis and progression (14,18,19). The activation

of the Hedgehog pathway affects the survival, proliferation, apoptosis, migration and invasion of tumors (20-24). Therefore, to explore the mechanism by which K19 affects the progression and prognosis of pancreatic cancer, the effect of K19 on the Hedgehog pathway in pancreatic cancer was analyzed. As presented in Figs. 6A and S3A, knockdown of K19 downregulated the expression of Indian hedgehog (Ihh), transmembrane receptor patched (PTCH), G protein-coupled-like receptor smoothened (SMO) and Gli1-the key proteins of the Hedgehog pathway; by contrast, overexpression of K19 upregulated their expression in pancreatic cancer cells (Figs. 6B and S3B). Of note, the expression of Ihh, PTCH, SMO and Gli1 in pancreatic cancer tissues with positive K19 expression was also upregulated as compared with that in pancreatic cancer tissues with

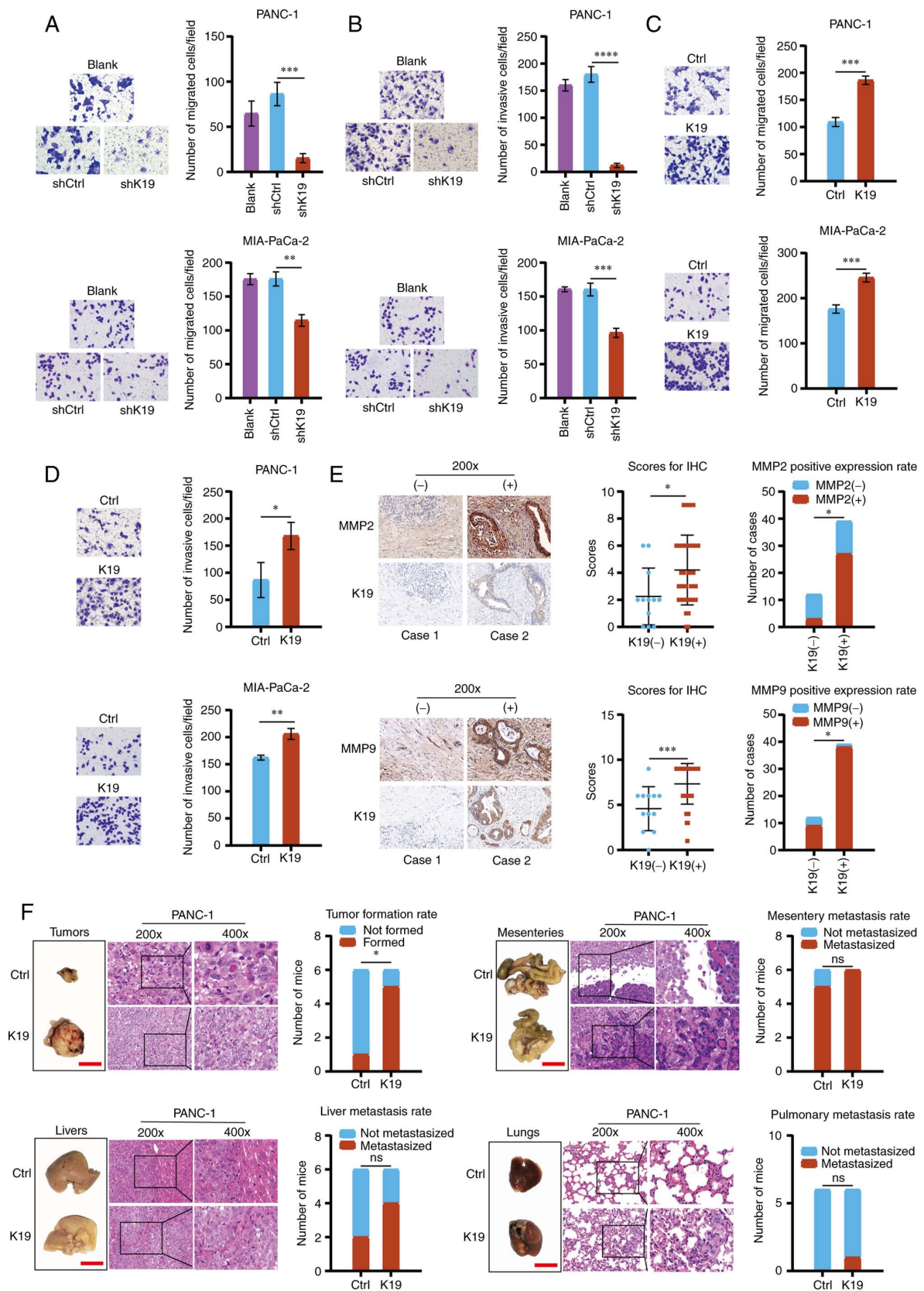


Figure 5. K19 promotes pancreatic cancer metastasis *in vitro* and *in vivo*. (A) Knockdown of K19 inhibited the migration of PANC-1 and MIA-PaCa-2 cells (magnification, x200). (B) Knockdown of K19 inhibited the invasion of PANC-1 and MIA-PaCa-2 cells (magnification, x200). (C) Overexpression of K19 promoted the migration of PANC-1 and MIA-PaCa-2 cells (magnification, x200). (D) Overexpression of K19 promoted the invasion of PANC-1 and MIA-PaCa-2 cells (magnification, x200). The migration and invasion of pancreatic cancer cells with knockdown of K19 and overexpression of K19 was detected by Transwell migration and invasion assays. These experiments were repeated three times. (E) K19 upregulated the expression of MMP2 and MMP9 in pancreatic cancer tissues (magnification, x200). The expression of MMP2 and MMP9 in pancreatic cancer tissues with K19 positive and K19 negative was detected by immunohistochemistry. (F) Overexpression of K19 promoted the tumorigenesis and metastasis of peritoneal metastasis tumors in the mice injected with PANC-1 cells that overexpress K19 (magnification, x200 in left panels and x400 in magnified windows to the right; scale bar in tumor/organ images, 1 cm). * $P < 0.05$, ** $P < 0.01$, *** $P < 0.001$, **** $P < 0.0001$; ns, no significance; K19, keratin 19; Ctrl, control; sh, short hairpin RNA.

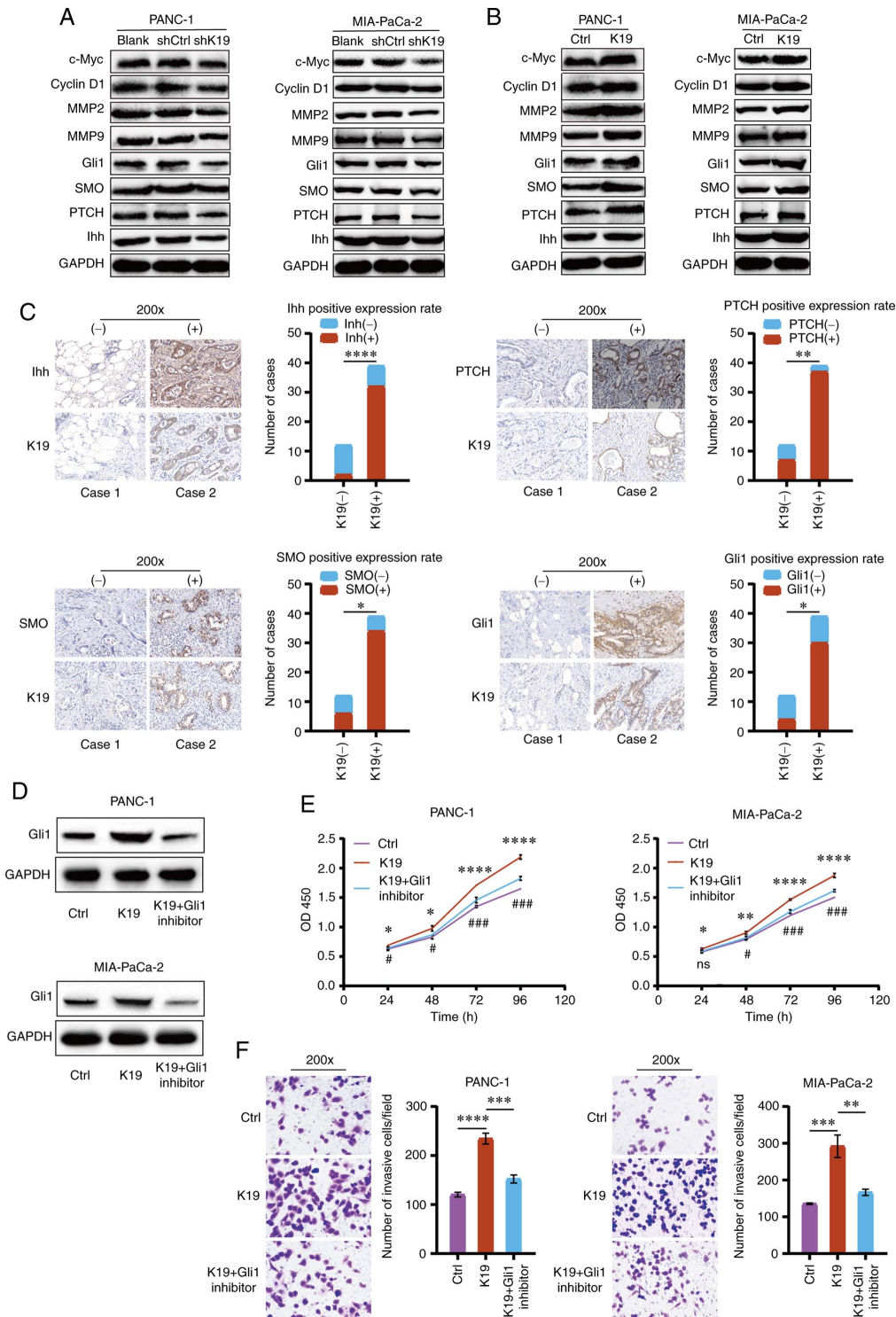


Figure 6. K19 activates the Hedgehog pathway and promotes the proliferation and metastasis of pancreatic cancer. (A) Knockdown of K19 downregulated the expression of Ihh, PTCH, SMO, Gli1, c-Myc, CyclinD1, MMP2 and MMP9 in PANC-1 and MIA-PaCa-2 cells. (B) Overexpression of K19 upregulated the expression of Ihh, PTCH, SMO, Gli1, c-Myc, CyclinD1, MMP2 and MMP9 in PANC-1 and MIA-PaCa-2 cells. The expression of Ihh, PTCH, SMO, Gli1, c-Myc, CyclinD1, MMP2 and MMP9 in pancreatic cancer cells with knockdown of K19 and overexpression of K19 was detected by western blot. (C) K19 upregulated the expression of Ihh, PTCH, SMO and Gli1 in pancreatic cancer tissues (magnification, x200). The expression of Ihh, PTCH, SMO and Gli1 in pancreatic cancer tissues with K19 positive and K19 negative was detected by immunohistochemistry. (D) Overexpression of K19 upregulated the expression of Gli1 in PANC-1 and MIA-PaCa-2 cells, while Gli1 inhibitor reversed it. The expression of Gli1 in pancreatic cancer cells in K19 overexpression group, K19 overexpression + Gli1 inhibitor group and control group was detected by western blot analysis. (E) Overexpression of K19 promoted the proliferation of PANC-1 and MIA-PaCa-2 cells, while Gli1 inhibitor reversed it. The proliferation of pancreatic cancer cells in K19 overexpression group, K19 overexpression + Gli1 inhibitor group and control group was detected by a Cell Counting Kit-8 assay. These experiments were repeated three times. (F) Overexpression of K19 promoted the invasion of PANC-1 and MIA-PaCa-2 cells, while Gli1 inhibitor reversed it (magnification, x200). Invasion of pancreatic cancer cells in K19 overexpression group, K19 overexpression + Gli1 inhibitor group and control group was detected by a Transwell invasion assay. These experiments were repeated three times. * $P < 0.05$, ** $P < 0.01$, *** $P < 0.001$, **** $P < 0.0001$, K19 overexpression vs. control group or as indicated; # $P < 0.05$, ### $P < 0.001$, K19 overexpression + Gli1 inhibitor vs. K19 overexpression group. ns, no significance. K19, keratin 19; Ctrl, control; sh, short hairpin RNA; OD450, optical density at 450 nm; PTCH, transmembrane receptor patched; SMO, G protein-coupled-like receptor smoothened; Ihh, Indian hedgehog; Gli1, glioma-associated oncprotein 1.

negative K19 expression (Fig. 6C). These data indicated that K19 activated the Hedgehog pathway in pancreatic cancer.

It is generally thought that Gli1 is a reliable marker for the activation of the Hedgehog pathway (25). Therefore, to observe whether the mechanism by which K19 promotes pancreatic cancer progression is through activating the Hedgehog pathway, a Gli1 inhibitor was used to block the Hedgehog pathway. As demonstrated in Fig. 6D, overexpression of K19 upregulated the expression of Gli1, while Gli1 inhibitor reversed this effect. It was then observed that overexpression of K19 promoted the proliferation and invasion of pancreatic cancer, while Gli1 inhibitor reversed these effects (Fig. 6E and F). Of note, knockdown of K19 downregulated the expression of Ihh, PTCH, SMO and Gli1, and also downregulated the expression of c-Myc, CyclinD1, MMP2 and MMP9 in pancreatic cancer cells (Figs. 6A and S3A). Overexpression of K19 upregulated the expression of Ihh, PTCH, SMO and Gli1, and also upregulated the expression of c-Myc, CyclinD1, MMP2 and MMP9 in pancreatic cancer cells (Figs. 6B and S3B). Collectively, these data indicated that K19 activated the Hedgehog pathway to promote pancreatic cancer progression. In other words, the mechanism by which K19 promoted pancreatic cancer progression was through the activation of the Hedgehog pathway.

Discussion

Although previous studies have indicated that tumors expressing K19 have stronger invasiveness and worse prognosis (7,8), the function and mechanism of K19 in pancreatic cancer progression and prognosis remain largely elusive. In the present study, it was indicated that K19 has a critical role in promoting pancreatic cancer progression and to be associated with poor prognosis. Specifically, K19 was significantly overexpressed in pancreatic cancer and an indicator of poor prognosis. Furthermore, K19 promoted pancreatic cancer proliferation, tumorigenesis and metastasis, and inhibited its apoptosis. Mechanistically, these effects were mediated through activating the Hedgehog pathway.

CyclinD1 and c-Myc inhibit tumor cell apoptosis, promote their proliferation and cell cycle progression, and have a key role in tumorigenesis (11,12,26-28). Of note, in the present study, it was indicated that K19 upregulated the expression of CyclinD1 and c-Myc in pancreatic cancer, promoted pancreatic cancer proliferation, cell cycle progression, tumorigenesis and development, and inhibited its apoptosis. Reducing extracellular matrix and basement membrane is the key mechanism of tumor invasion and metastasis. MMP2 and MMP9 may reduce extracellular matrix and basement membrane and have a key role in tumor invasion and metastasis (29,30). Downregulating or inhibiting MMP2 and MMP9 may inhibit tumor migration and invasion (31,32). Of note, in the present study, it was indicated that K19 upregulated MMP2 and MMP9 in pancreatic cancer and promoted pancreatic cancer cell migration, invasion and metastasis. These data indicated that K19 may promote pancreatic cancer proliferation and metastasis to promote pancreatic cancer progression, at least in part via enhancing the expression of CyclinD1, c-Myc, MMP2 and MMP9.

The Hedgehog pathway has a crucial role in pancreatic cancer tumorigenesis and development (18,33). The activation of the Hedgehog pathway affects the survival, proliferation,

apoptosis, migration and invasion of tumors (20-24). Ihh, PTCH, SMO and Gli1 are the key proteins of the Hedgehog pathway (19,34). The Hedgehog pathway is regulated by the Hedgehog pathway ligands PTCH and SMO. When the ligands [Sonic hedgehog (Shh), Ihh and desert hedgehog] are combined with PTCH (PTCH1 and PTCH2), SMO increases and releases Gli1, Gli2 and Gli3 transcription factors, which promote transcription of Gli1, Gli2 and Gli3. As a result, the Hedgehog pathway is activated (15,22,35). Therefore, to investigate the mechanism by which K19 affects the progression and prognosis of pancreatic cancer, the expression of Ihh, PTCH, SMO and Gli1 in pancreatic cancer was observed. Of note, it was indicated that K19 upregulated the expression of Ihh, PTCH, SMO and Gli1 in pancreatic cancer tissues and cells. This finding indicated that K19 activated the Hedgehog pathway. Furthermore, it was found that the changes of CyclinD1, c-Myc, MMP2 and MMP9 were consistent with those of Ihh, PTCH, SMO and Gli1. K19 upregulated the expression of Ihh, PTCH, SMO and Gli1 in pancreatic cancer tissues and cells, and also upregulated the expression of CyclinD1, c-Myc, MMP2 and MMP9. These findings suggest that K19 promotes pancreatic cancer proliferation and metastasis through the activation of the Hedgehog pathway. Furthermore, it is generally thought that Gli1 is a reliable marker for the activation of the Hedgehog pathway (25). Therefore, to examine whether K19 promotes pancreatic cancer progression through activating the Hedgehog pathway, a Gli1 inhibitor was used to block the Hedgehog pathway. It was indicated that Gli1 inhibitor reversed pancreatic cancer proliferation and invasion induced by overexpression of K19. Collectively, these data suggest that the mechanism by which K19 promotes the progression and poor prognosis of pancreatic cancer is through the activation of the Hedgehog pathway.

Bcl-2 expression is related to the activation of the Hedgehog pathway in pancreatic cancer (15). The Hedgehog pathway key protein Shh inhibits apoptosis through upregulating Bcl-2 expression (36). Upregulation of Gli1 may upregulate Bcl-2 (37). The Hedgehog pathway regulates the survival of tumor cells by regulating Bcl-2 expression (38). Of note, in the present study, it was indicated that K19 upregulated the expression of Bcl-2 in pancreatic cancer tissues and cells, inhibited their apoptosis and activated the Hedgehog pathway. These data suggest that K19 activates the Hedgehog pathway to upregulate Bcl-2 expression and inhibit apoptosis in pancreatic cancer. This is consistent with previous studies (15,36).

In addition, in the present study, intraperitoneal injection instead of tail vein injection was chosen when constructing a metastatic tumor model, mainly because the intraperitoneal metastatic tumor model is more similar to the clinical characteristics of pancreatic cancer (39,40). In the subcutaneously transplanted tumor model, tumor growth was observed for a long time, mainly because the number of cells injected was low, so that the tumor grew slowly.

Of note, the present study also had certain limitations. First, it remains insufficiently clear how K19 activates the Hedgehog pathway to promote progression and poor prognosis of pancreatic cancer. Furthermore, it remains to be investigated whether patients with high K19 expression may benefit from chemotherapy and whether any drug may downregulate and inhibit

K19 in pancreatic cancer to improve progression and prognosis of pancreatic cancer. These topics are the areas that are currently being investigated or will be investigated in the future.

In conclusion, K19 promotes pancreatic cancer progression and poor prognosis. The mechanism involves the activation of the Hedgehog pathway. K19 may be a novel molecular target for pancreatic cancer treatment.

Acknowledgements

The authors are grateful to Professor Ting Wu from the School of Medicine, Xiamen University (Xiamen, China) for her guidance and help with this research work.

Funding

This work was supported by grants from the Natural Science Foundation of Guizhou Province [grant no. Qian ke he cheng guo (2019) 4444 to CZ], the Beijing Medical and Health Public Welfare Foundation (grant no. YWJKJJHKYJJ-B184054 to CZ), the Key Project of the Science and Technology Ministry of China (grant no. 2017ZX10203206-005-002 to WL) and the Young and Middle-Aged Backbone Talent Training Program of Fujian Health Commission (grant no. 2021GGB036 to ML).

Availability of data and materials

The datasets used and/or analyzed during the current study are available from the corresponding authors on reasonable request.

Authors' contributions

CZ contributed to the design, implementation and execution of the experiments; acquisition, analysis and interpretation of data; and writing the manuscript. YX, YR and ML contributed to the completion of the experiments and acquisition of data. XG and WL contributed to the design of the experiments, the interpretation of data and the revision of the manuscript critically for important intellectual content. CZ and WL checked and approved the authenticity of the raw data. All authors have read and approved the final manuscript.

Ethics approval and consent to participate

All patients provided informed consent for the surgical procedure and the obtainment/use of their sample and clinical data for research. The study received approval from the Ethics Committee of Guizhou Provincial People's Hospital [Guiyang, China; no. (2021)253] and was conducted in line with the principles of the Helsinki declaration. All experimental procedures involving animals were conducted in accordance with animal protocols approved by the Laboratory Animal Center of Xiamen University (Xiamen, China), which was in line with the principles of the ARRIVE guidelines.

Patient consent for publication

Not applicable.

Competing interests

The authors declare that they have no competing interests.

References

- Mizrahi JD, Surana R, Valle JW and Shroff RT: Pancreatic cancer. *Lancet* 395: 2008-2020, 2020.
- Jain T and Dudeja V: The war against pancreatic cancer in 2020-advances on all fronts. *Nat Rev Gastroenterol Hepatol* 18: 99-100, 2021.
- Bhave P, Pallan L, Long GV, Menzies AM, Atkinson V, Cohen JV, Sullivan RJ, Chiarion-Sileni V, Nyakas M, Kahler K, *et al*: Melanoma recurrence patterns and management after adjuvant targeted therapy: A multicentre analysis. *Br J Cancer* 124: 574-580, 2021.
- Chan A, Moy B, Mansi J, Ejlersen B, Holmes FA, Chia S, Iwata H, Gnant M, Loibl S, Barrios CH, *et al*: Final efficacy results of neratinib in HER2-positive hormone receptor-positive early-stage breast cancer from the phase III ExteNET trial. *Clin Breast Cancer* 21: 80-91.e7, 2021.
- Garcia Campelo MR, Lin HM, Zhu Y, Pérol M, Jahanzeb M, Popat S, Zhang P and Camidge DR: Health-related quality of life in the randomized phase III trial of brigatinib vs crizotinib in advanced ALK inhibitor-naïve ALK + non-small cell lung cancer (ALTA-1L). *Lung Cancer* 155: 68-77, 2021.
- Rhee H, Kim HY, Choi JH, Woo HG, Yoo JE, Nahm JH, Choi JS and Park YN: Keratin 19 expression in hepatocellular carcinoma is regulated by fibroblast-derived HGF via a MET-ERK1/2-API and SP1 axis. *Cancer Res* 78: 1619-1631, 2018.
- Kim H, Choi GH, Na DC, Ahn EY, Kim GI, Lee JE, Cho JY, Yoo JE, Choi JS and Park YN: Human hepatocellular carcinomas with 'Stemness'-related marker expression: Keratin 19 expression and a poor prognosis. *Hepatology* 54: 1707-1717, 2011.
- Kawai T, Yasuchika K, Ishii T, Katayama H, Yoshitoshi EY, Ogiso S, Kita S, Yasuda K, Fukumitsu K, Mizumoto M, *et al*: Keratin 19, a cancer stem cell marker in human hepatocellular carcinoma. *Clin Cancer Res* 21: 3081-3091, 2015.
- Livak KJ and Schmittgen TD: Analysis of relative gene expression data using real-time quantitative PCR and the 2(-Delta Delta C(T)) method. *Methods* 25: 402-408, 2001.
- Hu S, Chen Z, Gu J, Tan L, Zhang M and Lin W: TLE2 is associated with favorable prognosis and regulates cell growth and gemcitabine sensitivity in pancreatic cancer. *Ann Transl Med* 8: 1017, 2020.
- Wang XK, Zhang YW, Wang CM, Li B, Zhang TZ, Zhou WJ, Cheng LJ, Huo MY, Zhang CH and He YL: METTL16 promotes cell proliferation by up-regulating cyclin D1 expression in gastric cancer. *J Cell Mol Med* 25: 6602-6617, 2021.
- Zhao R, Liu Y, Wu C, Li M, Wei Y, Niu W, Yang J, Fan S, Xie Y, Li H, *et al*: BRD7 promotes cell proliferation and tumor growth through stabilization of c-Myc in colorectal cancer. *Front Cell Dev Biol* 9: 659392, 2021.
- Warren CFA, Wong-Brown MW and Bowden NA: BCL-2 family isoforms in apoptosis and cancer. *Cell Death Dis* 10: 177, 2019.
- Edlich F: BCL-2 proteins and apoptosis: Recent insights and unknowns. *Biochem Biophys Res Commun* 500: 26-34, 2018.
- Chen XL, Cheng QY, She MR, Wang Q, Huang XH, Cao LQ, Fu XH and Chen JS: Expression of sonic hedgehog signaling components in hepatocellular carcinoma and cyclopamine-induced apoptosis through Bcl-2 downregulation in vitro. *Arch Med Res* 41: 315-323, 2010.
- Gupta GP, Nguyen DX, Chiang AC, Bos PD, Kim JY, Nadal C, Gomis RR, Manova-Todorova K and Massagué J: Mediators of vascular remodelling co-opted for sequential steps in lung metastasis. *Nature* 446: 765-770, 2007.
- Hiratsuka S, Nakamura K, Iwai S, Murakami M, Itoh T, Kijima H, Shipley JM, Senior RM and Shibuya M: MMP9 induction by vascular endothelial growth factor receptor-1 is involved in lung-specific metastasis. *Cancer Cell* 2: 289-300, 2002.
- Bausch D, Fritz S, Bolm L, Wellner UF, Fernandez-Del-Castillo C, Warshaw AL, Thayer SP and Liss AS: Hedgehog signaling promotes angiogenesis directly and indirectly in pancreatic cancer. *Angiogenesis* 23: 479-492, 2020.
- Richtig G, Aigelsreiter AM, Asslaber M, Weiland T, Pichler M, Eberhard K, Sygulla S, Schauer S, Hoefler G and Aigelsreiter A: Hedgehog pathway proteins SMO and GLI expression as prognostic markers in head and neck squamous cell carcinoma. *Histopathology* 75: 118-127, 2019.

20. Feng J, Rao M, Wang M, Liang L, Chen Z, Pang X, Lu W and Sun Z: Triptolide suppresses pancreatic cancer cell proliferation by inhibiting hedgehog signaling pathway activity. *Sci China Life Sci* 62: 1409-1412, 2019.
21. Lospinoso Severini L, Quaglio D, Basili I, Ghirga F, Bufalieri F, Caimano M, Balducci S, Moretti M, Romeo I, Loricchio E, *et al*: A Smo/Gli multitarget hedgehog pathway inhibitor impairs tumor growth. *Cancers (Basel)* 11: 1518, 2019.
22. Wu X, Xiao S, Zhang M, Yang L, Zhong J, Li B, Li F, Xia X, Li X, Zhou H, *et al*: A novel protein encoded by circular SMO RNA is essential for Hedgehog signaling activation and glioblastoma tumorigenicity. *Genome Biol* 22: 33, 2021.
23. Yang C, Zheng X, Ye K, Sun Y, Lu Y, Fan Q and Ge H: miR-135a inhibits the invasion and migration of esophageal cancer stem cells through the Hedgehog signaling pathway by targeting Smo. *Mol Ther Nucleic Acids* 19: 841-852, 2020.
24. Guimaraes VSN, Vidal MTA, de Faro Valverde L, de Oliveira MG, de Oliveira Siquara da Rocha L, Coelho PLC, Soares FA, de Freitas Souza BS, Bezerra DP, Coletta RD, *et al*: Hedgehog pathway activation in oral squamous cell carcinoma: Cancer-associated fibroblasts exhibit nuclear GLI-1 localization. *J Mol Histol* 51: 675-684, 2020.
25. Doheny D, Manore SG, Wong GL and Lo HW: Hedgehog signaling and truncated GLI1 in cancer. *Cells* 9: 2114, 2020.
26. Montalto FI and De Amicis F: Cyclin D1 in cancer: A molecular connection for cell cycle control, adhesion and invasion in tumor and stroma. *Cells* 9: 2648, 2020.
27. Yenmiş G, Beşli N, Yaprak Saraç E, Hocaoglu Emre FS, Şenol K and Kanıgür G: Metformin promotes apoptosis in primary breast cancer cells by downregulation of cyclin D1 and upregulation of P53 through an AMPK-alpha independent mechanism. *Turk J Med Sci* 51: 826-834, 2021.
28. Zhong Y, Yang L, Xiong F, He Y, Tang Y, Shi L, Fan S, Li Z, Zhang S, Gong Z, *et al*: Long non-coding RNA AFAP1-AS1 accelerates lung cancer cells migration and invasion by interacting with SNIP1 to upregulate c-Myc. *Signal Transduct Target Ther* 6: 240, 2021.
29. Mondal S, Adhikari N, Banerjee S, Amin SA and Jha T: Matrix metalloproteinase-9 (MMP-9) and its inhibitors in cancer: A minireview. *Eur J Med Chem* 194: 112260, 2020.
30. Ren F, Tang R, Zhang X, Madushi WM, Luo D, Dang Y, Li Z, Wei K and Chen G: Overexpression of MMP family members functions as prognostic biomarker for breast cancer patients: A systematic review and meta-analysis. *PLoS One* 10: e0135544, 2015.
31. Zhang J, Wang R, Cheng L and Xu H: Celestrol inhibit the proliferation, invasion and migration of human cervical HeLa cancer cells through down-regulation of MMP-2 and MMP-9. *J Cell Mol Med* 25: 5335-5338, 2021.
32. Chuang YC, Hsieh MC, Lin CC, Lo YS, Ho HY, Hsieh MJ and Lin JT: Pinosylvin inhibits migration and invasion of nasopharyngeal carcinoma cancer cells via regulation of epithelial-mesenchymal transition and inhibition of MMP-2. *Oncol Rep* 46: 143, 2021.
33. Niyaz M, Khan MS, Wani RA, Shah OJ and Mudassar S: Sonic Hedgehog protein is frequently up-regulated in pancreatic cancer compared to colorectal cancer. *Pathol Oncol Res* 26: 551-557, 2020.
34. Mohd Ariffin K, Abd Ghani F, Hussin H, Md Said S, Yunus R, Veerakumarasivam A and Abdullah MA: Hedgehog signalling molecule, SMO is a poor prognostic marker in bladder cancer. *Malays J Pathol* 43: 49-54, 2021.
35. Kasiri S, Chen B, Wilson AN, Reczek A, Mazambani S, Gadhvi J, Noel E, Marriam U, Mino B, Lu W, *et al*: Stromal Hedgehog pathway activation by IHH suppresses lung adenocarcinoma growth and metastasis by limiting reactive oxygen species. *Oncogene* 39: 3258-3275, 2020.
36. Huang H, Yu H, Lin L, Chen J and Zhu P: Protective effect of sonic hedgehog against oxidized low-density lipoprotein-induced endothelial apoptosis: Involvement of NF-κB and Bcl-2 signaling. *Int J Mol Med* 45: 1864-1874, 2020.
37. Bigelow RL, Chari NS, Uden AB, Spurgers KB, Lee S, Roop DR, Toftgard R and McDonnell TJ: Transcriptional regulation of bcl-2 mediated by the sonic hedgehog signaling pathway through gli-1. *J Biol Chem* 279: 1197-1205, 2004.
38. Han ME, Lee YS, Baek SY, Kim BS, Kim JB and Oh SO: Hedgehog signaling regulates the survival of gastric cancer cells by regulating the expression of Bcl-2. *Int J Mol Sci* 10: 3033-3043, 2009.
39. Jiang YJ, Lee CL, Wang Q, Zhou ZW, Yang F, Jin C and Fu DL: Establishment of an orthotopic pancreatic cancer mouse model: Cells suspended and injected in Matrigel. *World J Gastroenterol* 20: 9476-9485, 2014.
40. Tang S, Hang Y, Ding L, Tang W, Yu A, Zhang C, Sil D, Xie Y and Oupický D: Intraperitoneal siRNA nanoparticles for augmentation of gemcitabine efficacy in the treatment of pancreatic cancer. *Mol Pharm* 18: 4448-4458, 2021.



This work is licensed under a Creative Commons Attribution-NonCommercial-NoDerivatives 4.0 International (CC BY-NC-ND 4.0) License.